Journal of Applied Sciences

ISSN 1812-5654

science alert

ANSInet
an open access publisher
http://ansinet.com

Journal of Applied Sciences 13 (7): 1073-1079, 2013
ISSN 1812-5654 / DOI: 10.3923/jas.2013.1073.1079

CFD Simulating to Compare Tangential-inlet Swirl Nozzle with Coaxial Nozzle on Internal Flow for Preparing Nano-drug in SEDS Process

[1,2]Kefeng Xiao, [1]Zhihui Hao and [1]Leilei Wang
[1]Laboratory of Bio-pharmacy of Agricultural,
College of Chemistry and Pharmaceutical Science, Qingdao Agricultural University,
Qingdao, 266109, China
[2]School of Mechanical Engineering, Shandong University, Jinan, 250061, China

Abstract: The comparison on the performance between tangential-inlet swirl nozzle and coaxial nozzle was conducted by Computational Fluid Dynamics (CFD) simulation. The two nozzles were special for the preparation of nano-drug in Solution enhanced dispersion by supercritical fluid (SEDS) process. Turbulent intensity, velocity magnitude and volume fraction of ethanol were selected to act as the parameters to be compared. The results of CFD simulation indicate that, on the one hand, both coaxial nozzle and tangential-inlet swirl nozzle can meet the requirement of preparing nano-drug in SEDS process and have their advantages. Coaxial nozzle can prepare particles with more even size distribution than tangential-inlet swirl nozzle. And tangential-inlet swirl nozzle, with more merits, can produce higher turbulence intensity on the boundary layer which prevents the crystal nuclei precipitated from adhering on the inner wall. In additional, tangential-inlet swirl nozzle can produce higher velocity at outlet which can decrease the growth time of crystal nuclei so as to prepare superfine particles. On the other hand, both of the nozzles have their relative defects which should be improved in future study.

Key words: CFD simulation, SEDS, tangential-inlet swirl nozzle, coaxial nozzle, nano-drug

INTRODUCTION

The pharmaceutical industry aims at producing nano-drug for use in drugs administered by various routes including the inhalation and oral modes. For instance, application of aerosol powders enables fast, controlled delivery of drugs into the human lungs and then into the blood. To achieve optimal efficiency of therapy the drug has to be formulated into uniform microparticles of the appropriate size and shape (Henczka *et al*., 2005). The method of preparing nano-drug include High-gravity Anti-solvent Precipitation (HGAP) (Chen *et al*., 2006), Medium Milling (MM) (Ain-Ai and Gupta, 2008), Emulsification Method (EM) (Trotta *et al*., 2001), Crystallization by Supercritical Fluid Technology (CSFT) (Chen *et al*., 2012; Sheth *et al*., 2012) and so forth. The particles prepared by classical precipitation methods are non-uniform in size and particle size distribution is very wide. Use of supercritical fluids enables easier production of ultrafine (micro- or nanosized) powders with desired properties and precise control of particle size and morphology. Supercritical Fluids are easily separated from crystalline products providing clean and recyclable technologies (Henczka *et al*., 2005).

According to the different roles of supercritical fluid in crystallization process, CSFT is categorized into three types, including Supercritical Anti-solvent (SAS) (Lesoin *et al*., 2011), Rapid Expansion of Supercritical Solutions (RESS) (Chen *et al*., 2011) and Particles from Gas Saturated Solutions (PGSS) (Rodrigues *et al*., 2004). In all of these processes, oversaturation of drug solution generated in SCF is utilized to achieve drug recrystallization in order to prepare nano-drug crystal. However, their mechanisms are different. In the process of RESS, drug needs to be dissolved in supercritical CO_2 firstly and then sprays, crystallizes. Whereas, the solubility of many drugs in supercritical CO_2 (SC-CO_2) is very low or even near zero, which limit the use of RESS. PGSS process was useful mainly for impregnating active ingredients into polymer matrices. While in the process of SAS, drug need to be dissolved in certain kind of organic solvent and then the solution mixes with SC-CO_2 in nozzle. The solubility of solute in the solution decreases dramatically, consequently, the uniform particles of solute precipitate because of supersaturation and then spray out promptly forming nano-drug. Based on the principle of SAS, solution enhanced dispersion by supercritical fluid

Corresponding Author: Zhihui Hao, College of Chemistry and Pharmaceutical Science, Qingdao Agricultural University, Qingdao, 266109, China

(SEDS) has been developed. This process needs a nozzle with two passages to introduce SCF and a solution of active substance(s) in order to make these two fluids mix completely and to spray fiercely.

Nozzle is the key component of equipment for SEDS process. The reports about nozzle design frequently appear in literatures, such as capillary injection tubes (Reverchon *et al*., 2000), coaxial nozzles (Baldyga *et al*., 2010a), internal twin-fluid mixing nozzles (Ghaderi *et al*., 1999), jet-swirl nozzle (Jarmer *et al*., 2003), Tangential-inlet Swirl Nozzle (Xiao and Ma, 2007). All of above-mentioned mixing configurations are merely verified meeting the requirement of SEDS process. However, there are seldom comparisons among them on the important parameters of internal flow in the goal of distinguishing their relative advantages and disadvantages. In this study, CFD Simulation was utilized to compare on the important parameters of internal flow between tangential-inlet swirl nozzle and coaxial nozzle for preparing nano-drug in the same conditions so as to find the advantages of one nozzle compared to the other.

CFD SIMULATION

Nozzle structures and computational domain modeling: Bałdyga *et al*. (2010b) designed coaxial nozzle for preparing nano-drug in SEDS process. The structure and dimensions of this nozzle were shown in Fig. 1. There were three values for L_n in the literature. In this study, the value of L_n was 4 mm, one of that three. Supercritical CO_2 is introduced from an annular orifice and ethanol is introduced from a circular orifice. The flow directions of supercritical CO_2 and ethanol are the same and axial. The 3D geometrical computational domain of coaxial nozzle under consideration for CFD simulation is shown in Fig. 2a.

Xiao and Ma (2007) designed tangential-inlet swirl nozzle for preparing nano-drug in SEDS process. The structure and dimensions of the nozzle were shown in Fig. 3. The main feature of this nozzle is that solution and anti-solvent are injected, respectively from two tangential inlets and mixing of the jets occurs within the swirl chamber of the nozzle. The application of swirl flow plays the role of enhancing mixing because swirl flow produce strong shear stress, high turbulence and rapid mixing rates. The centrifugal force is imparted to the bulk liquid by a free vortex in the swirl chamber. The swirling liquid in the swirl chamber produce a swirling hollow-cone annular jet by passing through the outlet passage. Moreover, the strong shear stress can prevent particles precipitated from adhering in the inner wall of the nozzle. The 3D geometrical computational domain of this nozzle was shown in Fig. 2b.

The dimensions of these two kinds of nozzles are similar and both of the nozzles are designed for preparing nano-drug in SEDS process. In this study, the performance of these two nozzles was compared by comparing the important parameters of their internal flow by CFD simulation.

Governing equations: The continuity equation is defined as Eq. 1:

$$\frac{\partial(\rho u)}{\partial x}+\frac{\partial(\rho v)}{\partial y}+\frac{\partial(\rho w)}{\partial z}=0 \quad (1)$$

where u, v, w are, respectively the component of velocity vector in x, y and z direction. ρ is the density of the mixture. The momentum conservation equations are defined as Eq. 2-4:

$$\frac{\partial(\rho u)}{\partial t}+\mathrm{div}^{(\rho u\vec{u})}=\mathrm{div}\,(\mu \mathrm{grad}^{u})-\frac{\partial p}{\partial x}+S_u \quad (2)$$

$$\frac{\partial(\rho v)}{\partial t}+\mathrm{div}^{(\rho v\vec{u})}=\mathrm{div}\,(\mu \mathrm{grad}^{v})-\frac{\partial p}{\partial y}+S_v \quad (3)$$

$$\frac{\partial(\rho w)}{\partial t}+\mathrm{div}^{(\rho w\vec{u})}=\mathrm{div}\,(\mu \mathrm{grad}^{w})-\frac{\partial p}{\partial w}+S_w \quad (4)$$

where, S_u, S_v and S_w are the generalized source term of the momentum conservation equations.

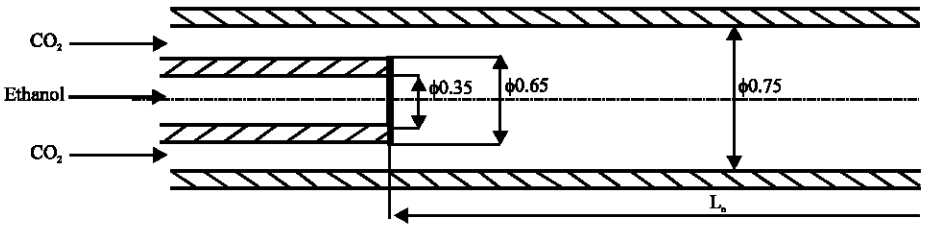

Fig. 1: Schematic diagram of structure and dimensions of coaxial nozzle (Baldyga *et al*., 2010a)

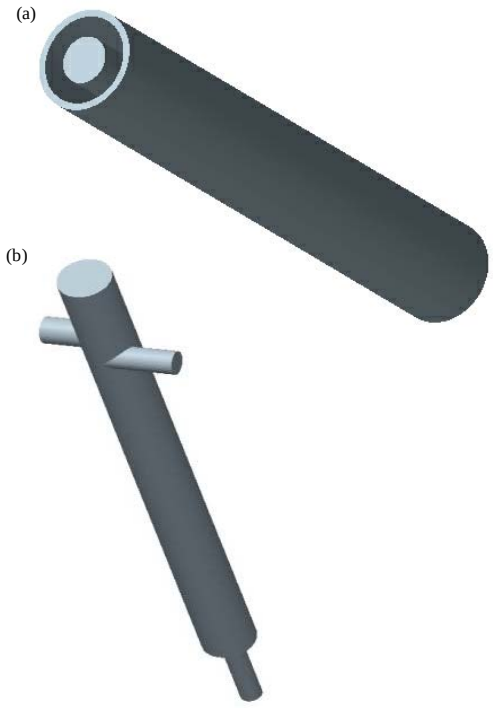

Fig. 2(a-b): The model of computational domain of the two nozzles, (a) Coaxial nozzle and (b) Tangential-inlet swirl nozzle

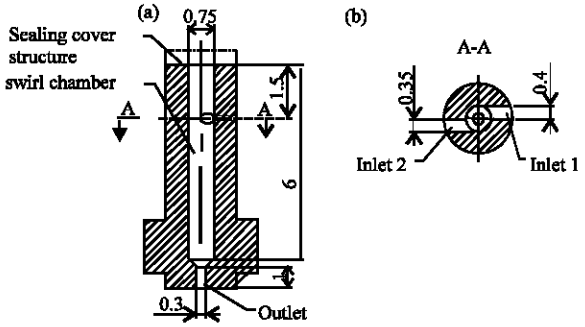

Fig. 3(a-b): Structure sketch of the tangential-inlet swirl nozzle, (a) A sectional view of the nozzle and (b) A-A cut of the nozzle

An energy conservation equation, as shown in Eq. 5, was utilized to take into account the effect of heat transfer on hydrodynamics:

$$\frac{\partial(\rho T)}{\partial t}+\mathrm{div}^{(\rho\vec{T})}=\mathrm{div}\left(\frac{k}{C_T}\mathrm{grad}^{T}\right)+S_T \quad (5)$$

where, C_p is isobaric specific heat capacity. T is temperature. k is heat transfer coefficient. S_T is viscous dissipation term.

Standard model was employed to simulate the turbulence of the flow in tangential-inlet swirl nozzle. The governing equation groups are shown as Eq. 6 and 7:

$$\frac{\partial(\rho k)}{\partial t}+\frac{\partial(\rho k u_i)}{\partial x_i}=\frac{\partial}{\partial x_i}\left[(\mu+\mu_t)\frac{\partial k}{\partial x_i}\right]+G_k-\rho\varepsilon \quad (6)$$

$$\frac{\partial(\rho\varepsilon)}{\partial t}+\frac{\partial(\rho\varepsilon u_i)}{\partial x_i}=\frac{\partial}{\partial x_i}\left[\left(\mu+\frac{\mu_t}{1.3}\right)\frac{\partial\varepsilon}{\partial x_i}\right]+\frac{1.44\varepsilon}{k}G_k-1.92\rho\frac{\varepsilon^2}{k} \quad (7)$$

Turbulent kinetic energy k can be calculated by Eq. 4:

$$k=\frac{3}{2}\left(\bar{u}_{ref}I\right)^2 \quad (8)$$

where, $\bar{u}_{ref}$ is the mean velocity at inlet, which can be calculated by mass flow rate. I is the turbulent intensity of inlet, which can be calculated by Eq. 5:

$$I = 0.16\,(R_{eDH})^{-1/8} \quad (9)$$

Turbulent dissipation rate ε was estimated by Eq. 6 and 7:

$$\varepsilon = 0.09^{3/4}\frac{k^{3/2}}{l} \quad (10)$$

$$l = 0.07L \quad (11)$$

where, k is turbulent kinetic energy, L is characteristic length, which can be calculated according to the equivalent diameter.

Numerical scheme: The CFD approach uses a numerical technique for solving the governing equations for a given flow geometry and boundary conditions. In this study, a commercial CFD code, Fluent 6.3, was selected to simulate the flow pattern through the two nozzles. In order to simulate the precipitation in a two-phase system, Eulerian model was chosen to act as Multiphase Model. Both SCF and solution were assumed as continuum phases. For turbulent flow calculations, the realizable k-∈ turbulence model was selected with standard wall functions. The phase coupled SIMPLE algorithm was utilized to achieve Pressure-velocity coupling. The first order upwind discretization schemes were employed to solve the volume fraction, the turbulence, the momentum equations and the energy equations. The solution was convergent when the scaled residuals were less than 1×10^{-3}.

Materials and operating parameters: Ethanol and SC-CO_2 were selected as solvent and anti-solvent, respectively

(Cardoso *et al*., 2008; Baldyga *et al*., 2010b). Because there was a little solute in the solution (Liu *et al*., 2011), it was assumed that the fluid in the nozzle include two phases. SC-CO_2 was selected as the primary phase and ethanol was the secondary phase. Because the pressure difference between inlet and outlet is small, the two-phase system was considered as incompressible in order to develop CFD simulations (Leybros *et al*., 2012; Moussiere *et al*., 2012). All fluid variations were considered to be isobaric at 10 Mpa.

Boundary conditions: For coaxial nozzle, as shown in Fig. 1, the inlet of CO_2 was inlet1 and the inlet of ethanol was inlet2. For tangential-inlet swirl nozzle, as shown in Fig. 3, the inlet1 was the inlet of SC-CO_2 and inlet2 was the inlet of ethanol. For both of the nozzles, in terms of the inlet boundary condition of inlet1, a simple mass flow inlet was selected and allowed to specify mass flow and temperature of SC-CO_2, turbulent kinetic energy, turbulent dissipation rate and initial volume fraction of ethanol. The mass flow and temperature of SC-CO_2 were 5.46×10^{-4} kg sec^{-1} and 363 K, respectively. The volume fraction of ethanol was zero.

For inlet2, the inlet boundary condition was designated to be velocity-inlet. The velocity magnitude was 0.5 m sec^{-1}. Turbulent intensity is 1% and hydraulic diameter is 0.35 mm. The temperature of inlet2 was 313 K. The pressure-outlet boundary condition was selected as the boundary condition of outlet. The pressure of outlet was set to be 8 Mpa. The conditions of pressure, temperature, mass flow rate and velocity magnitude used in this work were selected because they presented the best results regarding the morphology and the particle size distribution of the obtained particles (Baldyga *et al*., 2010a, b).

RESULTS AND DISCUSSION

Comparison of turbulent intensity at outlet: The contours of turbulent intensity at the outlet of these two nozzles were shown in Fig. 4. Turbulent intensity distribution on the diameter of the outlet of these two nozzles were shown in Fig. 5. As can be seen from Fig. 4a and 5a, the turbulent intensity on the outlet center of coaxial nozzle is 15% higher than that on the outlet edge. That because the flow in the nozzle is just like the flow in a tube and the resistance of boundary layer can not be ignored. On the contrary, for tangential-inlet swirl nozzle, the turbulent intensity on edge is higher than that on center as shown in Fig. 4b and 5b. That mainly because the fluids were introduced in the nozzle from tangential direction which counterweight the resistance of boundary layer. Moreover, the turbulent intensity in tangential-inlet swirl nozzle is far higher than that in coaxial nozzle. In SEDS process, high turbulent intensity is facilitated to mix SC-CO_2 fully with solution so as to form superfine particles. And particles are prone to adhere on the inner wall of nozzle so that the outlet is blocked. Therefore, high turbulent intensity on edge is more essential than that on center for nozzles. Consequently, from the aspect of turbulent

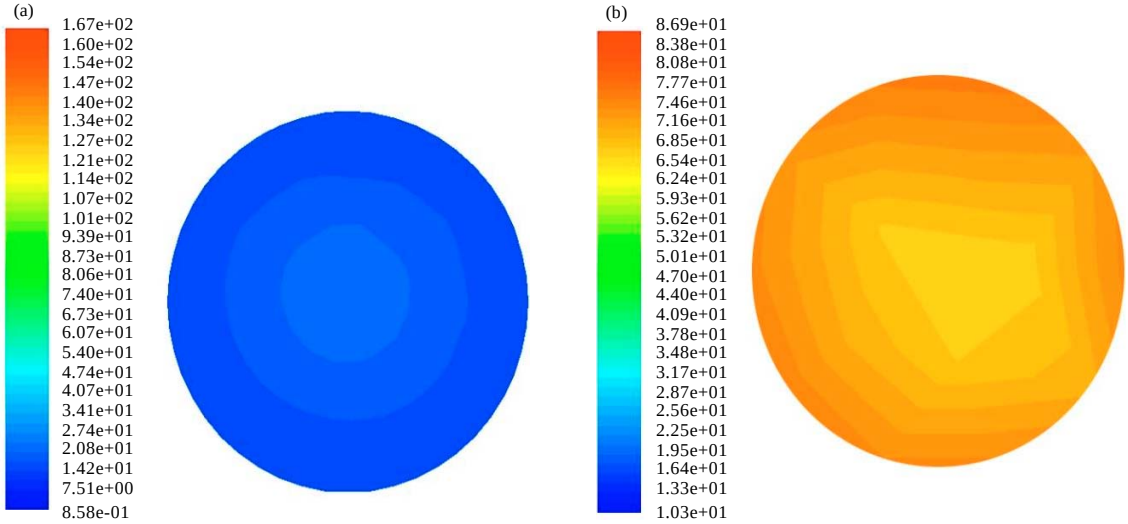

Fig. 4(a-b): Contours of turbulent intensity at the outlet of nozzle, (a) Coaxial nozzle and (b) Tangential-inlet swirl nozzle

intensity, the tangential-inlet swirl nozzle improved the distribution of turbulent intensity and outshined the coaxial nozzle.

Comparison of velocity magnitudes at outlet: The velocity magnitudes of the flow at outlet, influencing the growth time of crystal nuclei and particle size distribution, is an important parameter to indicate the performance of nozzle. The contours of velocity magnitudes at the outlet of the two nozzles were shown in Fig. 6. Velocity magnitudes distribution on the diameter of the outlet of the two nozzles was shown in Fig. 7. On the one hand, from the comparison of Fig. 6a and b, it can be concluded that the velocity magnitude distribution of coaxial nozzle is more even than that of tangential-inlet swirl nozzle. Even velocity magnitudes distribution is facilitated to control narrow particle size distribution. In this respect, the coaxial nozzle exceeds tangential-inlet swirl nozzle. On the other hand, from the comparison of Fig. 7a and b, it can be inferred that the velocity magnitudes on the diameter of tangential-inlet swirl nozzle are far higher than that of coaxial nozzle. High velocity can decrease the growth time of crystal nuclei, contributing to forming superfine particles. Consequently, the size of particle prepared by tangential-inlet swirl nozzle will be smaller than that of particle prepared by coaxial nozzle. From all above-mentioned CFD analysis, it can be conclude that tangential-inlet swirl nozzle can produce smaller particles, but the particle size distribution is not desired.

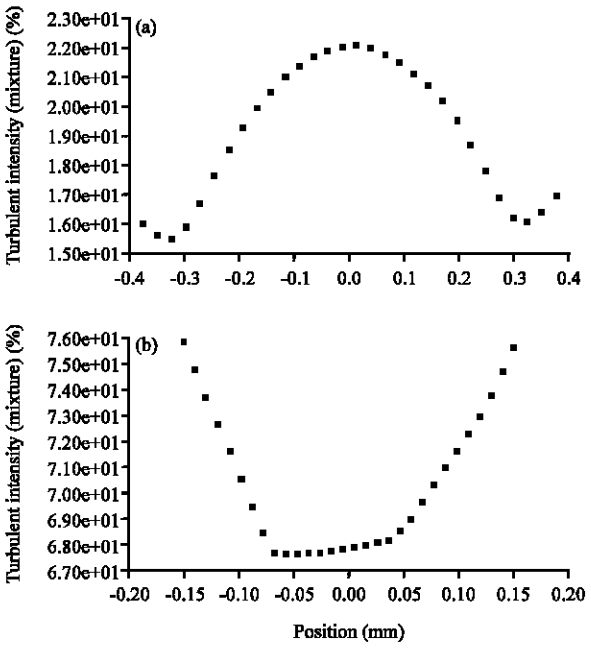

Fig. 5(a-b): Turbulent intensity distribution on the diameter of the outlet of the two nozzles, (a) Coaxial nozzle and (b) Tangential-inlet swirl nozzle

Comparison of volume fraction of ethanol in the nozzles: As shown in Fig. 8a and b, SC-CO_2 and ethanol began to mix in the upper part of these two nozzles and became entirely mixed in the lower part of these two nozzles. SC-CO_2 and ethanol was mixed by axial force in coaxial nozzle and by tangential force in tangential-inlet swirl nozzle. When the mixture reached outlet, SC-CO_2 had

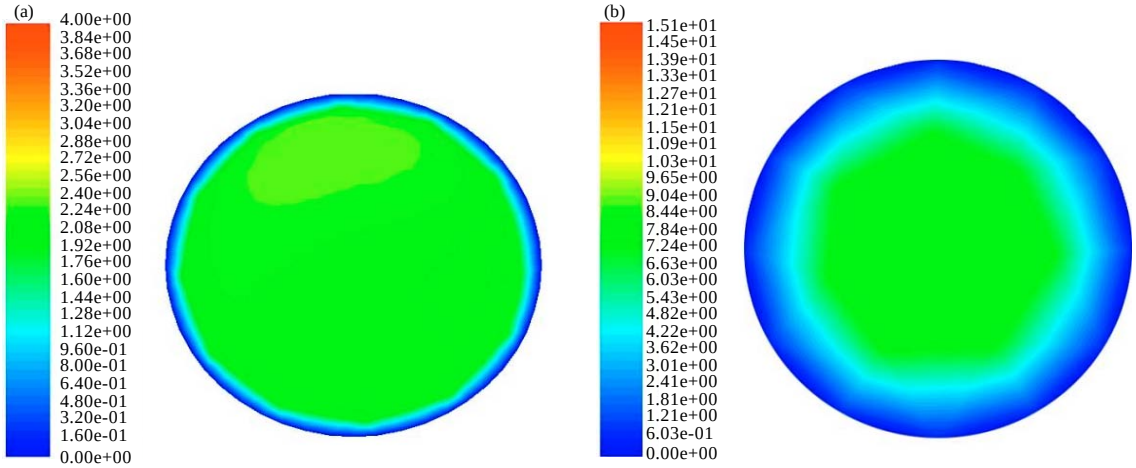

Fig. 6(a-b): Contours of velocity magnitudes at the outlet of the two nozzles, (a) Coaxial nozzle and (b) Tangential-inlet swirl nozzle

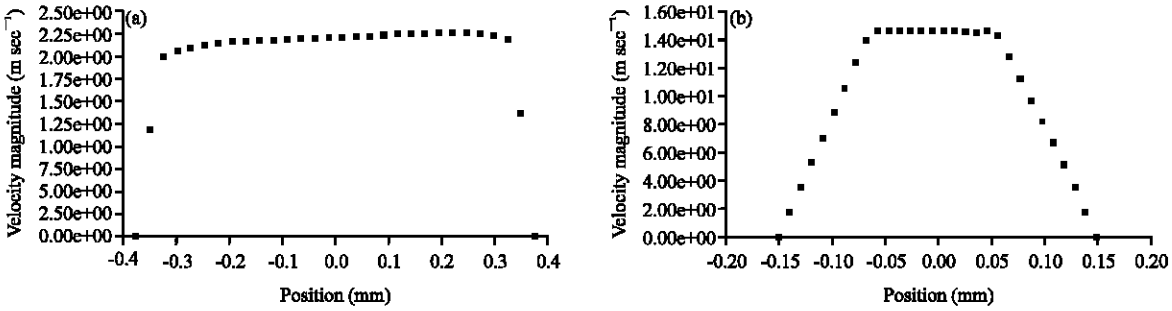

Fig. 7(a-b): Velocity magnitudes distribution on the diameter of the outlet of the two nozzles, (a) Coaxial nozzle and (b) Tangential-inlet swirl nozzle

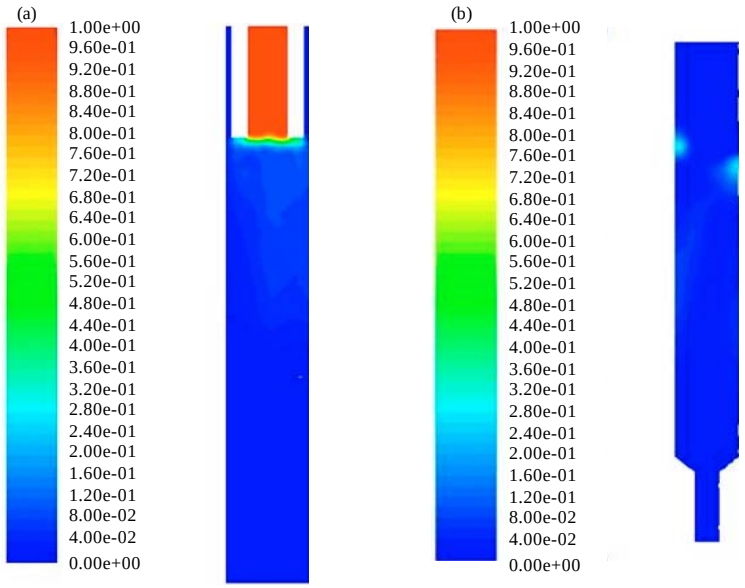

Fig. 8(a-b): Contours of volume fraction of ethanol on the longitudinal section of the two nozzles, (a) Coaxial nozzle and (b) Tangential-inlet swirl nozzle

given full play to the function of anti-solvent and the solute was precipitated. Therefore, from the aspect of mixing, both of the nozzles can meet the requirements of preparing nano-drug in SDES process. Although the structures are different, the results are similar.

CONCLUSION

In this study, the comparison on the performance between tangential-inlet swirl nozzle and coaxial nozzle was conducted by CFD simulating. Turbulent intensity, velocity magnitude and volume fraction of ethanol were selected to act as the parameters compared. From all above CFD simulations, on the one hand, it can be deduced that both coaxial nozzle and tangential-inlet swirl nozzle can meet the requirement of preparing nano-drug in SEDS process and have their advantages. Coaxial nozzle can prepare particles with more even size distribution than tangential-inlet swirl nozzle. And tangential-inlet swirl nozzle, with more merits, can produce higher turbulence intensity on the boundary layer which prevents the crystal nuclei precipitated from adhering on the inner wall. In additional, tangential-inlet swirl nozzle can produce higher velocity at outlet which can decrease the growth time of crystal nuclei so as to prepare superfine particles. On the other hand, both of the nozzles have their relative defects which should be improved in future study.

ACKNOWLEDGMENT

This work was financially supported by the National Key Technology R and D Program for the 12th Five-Year Plan (No. 2011BAD44B01).

REFERENCES

Ain-Ai, A. and P.K. Gupta, 2008. Effect of arginine hydrochloride and hydroxypropyl cellulose as stabilizers on the physical stability of high drug loading nanosuspensions of a poorly soluble compound. Int. J. Pharm., 351: 282-288.

Baldyga, J., D. Kubicki, B.Y. Shekunov and K.B. Smith, 2010a. Mixing effects on particle formation in supercritical fluids. Chem. Eng. Res. Design, 88: 1131-1141.

Baldyga, J., R. Czarnocki, B.Y. Shekunov and K.B. Smith, 2010b. Particle formation in supercritical fluids-Scale-up problem. Chem. Eng. Res. Des., 88: 331-341.

Cardoso, M.A.T., J.M.S. Cabral, A.M.F. Palavra and V. Geraldes, 2008. CFD analysis of Supercritical Antisolvent (SAS) micronization of minocycline hydrochloride. J. Supercrit. Fluids, 47: 247-258.

Chen, J.F., J.Y. Zhang, Z.G. Shen, J. Zhong and J. Yun, 2006. Preparation and characterization of amorphous cefuroxime axetil drug nanoparticles with novel technology: High-gravity antisolvent precipitation. Ind. Eng. Chem. Res., 45: 8723-8727.

Chen, A.Z., Z. Zhao, S.B. Wang, Y. Li, C. Zhao and Y.G. Liu, 2011. A continuous RESS process to prepare PLA-PEG-PLA microparticles. J. Supercrit. Fluids, 59: 92-97.

Chen, A.Z., L. Li, S.B. Wang, C. Zhao, Y.G. Liu, G.Y. Wang and Z. Zhao, 2012. Nanonization of methotrexate by solution-enhanced dispersion by supercritical CO_2. J. Supercrit. Fluids, 67: 7-13.

Ghaderi, R., P. Artursson and J. Carlfors, 1999. Preparation of biodegradable microparticles using solution-enhanced dispersion by supercritical fluids (SEDS). Pharm. Res., 16: 676-681.

Henczka, M., J. Baldyga and B.Y. Shekunov, 2005. Particle formation by turbulent mixing with supercritical antisolvent. Chem. Eng. Sci., 60: 2193-2201.

Jarmer, D.J., C.S. Lengsfeld and T.W. Randolph, 2003. Manipulation of particle size distribution of poly(L-lactic acid) nanoparticles with a jet-swirl nozzle during precipitation with a compressed antisolvent. J. Supercrit. Fluids, 27: 317-336.

Lesoin, L., C. Crampon, O. Boutin and E. Badens, 2011. Preparation of liposomes using the Supercritical Anti-Solvent (SAS) process and comparison with a conventional method. J. Supercrit. Fluids, 57: 162-174.

Leybros, A., R. Piolet, M. Ariane, H. Muhr, F. Bernard and F. Demoisson, 2012. CFD simulation of ZnO nanoparticle precipitation in a supercritical water synthesis reactor. J. Supercrit. Fluids, 70: 17-26.

Liu, Y., Y. P. Qu and W.Q. Wang, 2011. The structural design of nozzle in outer mixing mode for preparing superfine particles by SCF technology. Proceedings of the International Conference on Chemical Engineering and Advanced Materials, May 28-30, 2011, Changsha, China.

Moussiere, S., A. Roubaud, O. Boutin, P. Guichardon, B. Fournel and C. Joussot-Dubien, 2012. 2D and 3D CFD modelling of a reactive turbulent flow in a double shell supercritical water oxidation reactor. J. Supercrit. Fluids, 65: 25-31.

Reverchon, E., G. Della Porta, I. De Rosa, P. Subra and D. Letourneur, 2000. Supercritical antisolvent micronization of some biopolymers. J. Supercrit. Fluids, 18: 239-245.

Rodrigues, M., N. Peirico, H. Matos, E.G. de Azevedo, M.R. Lobato and A.J Almeida, 2004. Microcomposites theophylline/hydrogenated palm oil from a PGSS process for controlled drug delivery systems. J. Supercrit. Fluids, 29: 175-184.

Sheth, P., H. Sandhu, D. Singhal, W. Malick, N. Shah and M. Serpil Kislalioglu, 2012. Nanoparticles in the pharmaceutical industry and the use of supercritical fluid technologies for nanoparticle production. Curr. Drug Delivery, 9: 269-284.

Trotta, M., M. Gallarate, F. Pattarino and S. Morel, 2001. Emulsions containing partially water miscible solvents for the preparation of drug nanosuspensions. J. Control. Release, 76: 119-128.

Xiao, K.F. and X. Ma, 2007. Nozzle design of superfine particles preparation by using SEDS process. Liaoning Chem. Ind., 36: 486-488.